Scale-Model Vehicle Analysis Using an Off-the-Shelf Scale-Model Testing Apparatus

Richard T. O'Brien, Jr., *Member, IEEE*, Jenelle A. Piepmeier, *Member, IEEE*, Philip C. Hoblet, Steven R. Burns, and Charles E. George

Abstract— **A standard exercise treadmill is used to create a scale-model vehicle simulator. The motion of the treadmill beneath the scale-model vehicle simulates the motion of a full-size vehicle on a paved road. The Scale-Model Testing Apparatus incorporates off-the-shelf components and commercially available, scale-model vehicles which facilitates the development of the apparatus in an undergraduate setting. An overhead vision system provides a tether-free assessment of the vehicle's position and orientation. Dynamic similitude between the scale-model vehicle and an "average" full-size vehicle is achieved through a series of straightforward modifications to the scale-model vehicle. Preliminary results of longitudinal and lateral control designs are presented.**

I. INTRODUCTION

Automobile accidents injure close to ten million people a year [1]. One way to prevent automobile accidents is to design systems that assist the driver in emergency maneuvers. Unfortunately, there are few facilities where these systems can be tested using full-size automobiles. An alternative to expensive and potentially dangerous full-size testing is scale-model testing. An examination of the use of scale-models throughout history demonstrates that scale-models are technologically suitable alternatives to tests with full-size equipment [2].

A group at the University of Illinois created a scale-model vehicle simulator consisting of off-the-shelf and custom-built scale-model vehicles driven on modified treadmill [3]. The position and orientation of the vehicle on the treadmill are measured using a mechanical link to the vehicle [4]. Using this simulator, this group has investigated a number of issues in vehicle modeling and control including dynamic similitude analysis, driver-assistance steering control, and steering controller design using non-dimensional models [3], [5].

In this paper, the Scale-Model Testing Apparatus (SMTA) developed at the United States Naval Academy is presented. This apparatus is a simplified version of the platform developed at the University of Illinois. The objectives for the development of the SMTA are to use off-the-shelf components and to incorporate a vision feedback system. The use of off-the-shelf components and commercially available, scale-model vehicles facilitated the development of the apparatus for the undergraduate setting [6]. The vision system provides a tether-free assessment of the vehicle's position and orientation.

The SMTA (shown in Fig. 1) simulates the control of a full-scale vehicle by a human driver. The experimental apparatus provides a platform for investigating driver assistance control algorithms where the control system augments the driver's inputs to improve the performance of the vehicle. This experimental system consists of a treadmill, scale-model vehicle, MATLAB-based, real-time control system, and the aforementioned vision system. The treadmill simulates the road surface and vision system simulates the driver's visual measurements. The driver control systems regulate the motion of the scale-model vehicle by sending steering and throttle commands to the vehicle.

Given that the Naval Academy is an undergraduate institution, the goals for the SMTA are to incorporate vehicle control projects in the undergraduate control systems curriculum and to provide a research platform for students and faculty to investigate vehicle control issues. The SMTA has been developed through the course of two senior undergraduate thesis projects and promising preliminary results have been obtained. Specifically, a systematic process has been developed to achieve dynamic similitude between scale-model and full-size vehicles [7]. In the future, the SMTA and this process will be incorporated in a senior elective course on scale vehicle modeling and control.

The remainder of the paper is organized as follows. The major components of the experimental apparatus are presented in Section II. Section III contains a description of the scale-model vehicle and the process used to achieve dynamic similitude. Section IV provides an overview of the vehicle controllers and presents some preliminary results. Concluding remarks and directions for future work are included in Section V.

Manuscript received September 15, 2003. This work was supported in part by the Office Naval Research through the Naval Academy Office of Academic Research.

The authors are with the Systems Engineering Department, United States Naval Academy, Annapolis, MD 21402 USA (phone: 410-293-6118; fax: 410-293-2215; e-mail: riobrien@ usna.edu).

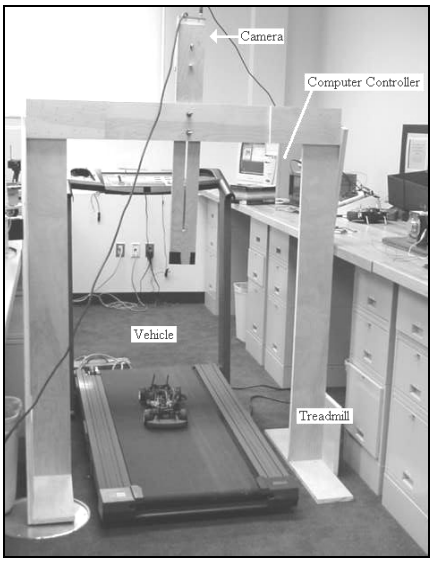

Fig. 1: Scale Model Testing Apparatus

II. EXPERIMENTAL APPARATUS

A standard exercise treadmill is used to create the road surface for the scale-model vehicle. The motion of the treadmill beneath the scale-model vehicle simulates the motion of a full-size vehicle on a paved road. Since the current research is focused on driver assistance control, the apparatus uses an overhead vision system to record the position and heading of the vehicle and to simulate the human driver. The vision system and the implementation of the control system are discussed in Sections III-B and III-C, respectively. The scale model vehicle and the modifications necessary to achieve dynamic similitude are discussed in Section IV. The control system design is discussed in V.

A. Vision System

A vision system is used to simulate a driver's visual feedback. Vehicle position and orientation are measured, and compared with a desired position or trajectory. To provide high contrast features, small LED lights are positioned at the four corners of the vehicle as shown in Fig. 2. Image capture and processing are performed on a DVT Series 600 Smartsensor digital camera. The camera computes the position and orientation of the car approximately every 180 ms, and the data are sent to the PC-based controller via RS-232 communications.

B. Control System

The steering and throttle inputs on the scale vehicle accept standard hobby servo inputs. The communication between the MATLAB- based, real-time controller and the vehicle is achieved using the SV203 controller board from Pontech, Inc. The board is capable of producing pulse-width modulated signals to drive the steering servo and the throttle controller.

III. SCALE VEHICLE

The scale-model vehicle is pre-assembled and available from HPI Racing, Inc. (http://www.hpiracing.com). The vehicle's features include four-wheel drive, four-wheel independent suspension, front and rear differentials, and a rugged, rigid structure that resembles a full size vehicle.

Comparisons of scale-model and full-size vehicles require that the two vehicles are dynamically similar. Dynamic similitude can be shown using the Buckingham-Pi Theorem replacing the dimensional physical parameters with dimensionless products and ratios (see [3]). Dimensionless groups, known as Pi groups, are formed from the ratios of physical parameters. Two systems are dynamically similar if the corresponding Pi groups are equal. The differences between the Pi groups of the scale-model and full-size vehicles are resolved by modifying the scale-model vehicle.

The lateral motion of the vehicle and the cornering properties of the tires are described using the bicycle model [8] and the Dugoff tire model [9], respectively. Following the development in [3], eight parameters governing the vehicle's lateral motion are selected from these models and organized into five Pi groups

$$\Pi_1 = \frac{a}{L} \qquad \Pi_2 = \frac{b}{L} \qquad \Pi_3 = \frac{C_{\alpha_f} L}{mU^2}$$

$$\Pi_4 = \frac{C_{\alpha_r} L}{mU^2} \qquad \Pi_5 = \frac{I_z}{mL^2}$$

where $C_{\alpha f}$ ($C_{\alpha r}$) denote the front (rear) cornering stiffness, a (b) denote the longitudinal distance from the front (rear) axle to the center of gravity, L denotes the longitudinal distance from the front axle to the rear axle, m denotes the mass, U denotes the longitudinal velocity, and I_z denotes the moment of inertia about the z-axis.

After measuring the parameters of the scale-model vehicle, the Pi groups are calculated. In order to achieve dynamic similitude, the Pi groups of the scale-model

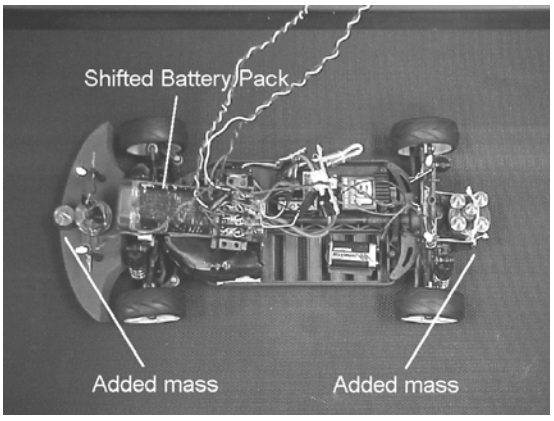

Fig. 2: Scale model vehicle with modifications to achieve dynamic Similitude

TABLE I
PI GROUPS FOR SCALE-MODEL AND FULL-SIZE VEHICLES

Vehicle\Pi Group	Π_1	Π_2	Π_3	Π_4	Π_5
1989 Escort	0.368	0.632	0.745	0.275	0.219
1980 LeSabre	0.443	0.557	0.738	0.587	0.257
1988 Ranger	0.421	0.578	0.884	0.644	0.239
1989 Wrangler	0.465	0.534	0.825	0.719	0.230
Original Scale vehicle	0.532	0.468	1.35	0.938	0.113
Modified Scale vehicle	0.405	0.595	0.812	0.564	0.230

vehicle are compared to the Pi groups of a number of full-size vehicles of various sizes, types, and manufacturers. Fig. 2 shows the scale-model vehicle after the required modifications were made to achieve dynamic similitude with an "average" full-size vehicle. The Pi groups for the "average" full-size vehicle take values within the range of values for a selection of full-size vehicles [10] (1989 Honda Escort, 1982 Honda Civic, 1983 Volkswagen Jetta, 1980 Buick La Sabre, 1983 Chevrolet S-10, 1988 Ford Ranger, 1987 Ford F-150, 1983 Chevrolet Blazer, 1989 Jeep Wrangler). A comparison of the Pi groups of the original and modified scale-model vehicles to selected full-size vehicles is shown in Table 1.

A. Center of Gravity

The first two Π groups, $\prod_1 = \frac{a}{L}$ and $\prod_2 = \frac{b}{L}$ are determined from the vehicle's center of gravity. For most full-sized vehicles, the center of gravity of is closer to the front axle than the rear axle due the placement of the engine. On the scale-model vehicle, the center of gravity is near the rear axle due to the placement of the motor and battery pack. In order to match the first two Pi groups of the scale-model vehicle with those of the "average" full-size vehicle, the center of gravity of the scale-model vehicle is shifted forward by moving the battery pack over the front axle as shown in Fig. 2.

B. Moment of Inertia

The moment of inertia about the z-axis of the scale-model vehicle, I_z, is found by approximating the vehicle's shape and weight distribution as shown in Fig. 3.

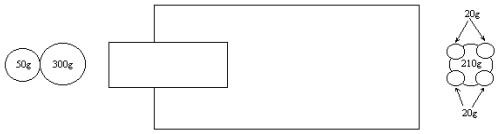

Fig. 3: Approximation of vehicle weight distribution (including added weight) for moment of inertia analysis

The Π_5 value for the scale-model vehicle is much smaller than the values for the full-size vehicles. Therefore, the scale-model vehicle must be modified in order to produce a greater I_z. This can be accomplished by adding mass to both the front and rear of the car so that Π_1 and Π_2 (i.e., the center of gravity) remain unchanged. The placement of the added mass on the scale-model vehicle is shown in Fig. 2.

C. Tires

Along with the vehicle parameters, the tire parameters must also be investigated in order to match the Pi groups and produce dynamic similitude between the scale-model vehicle and the full-size vehicles.

1) Cornering Stiffness

The Dugoff tire model assumes that the steering force, F_y, is linearly related to the slip angle, α, by $F_y = C_\alpha \alpha$. As a result, the cornering stiffness, C_α, is the only tire parameter that is needed. Two of the five Pi groups depend on cornering stiffness, $\Pi_3 = \frac{C_{\alpha_f} L}{mU^2}$ and $\Pi_4 = \frac{C_{\alpha_r} L}{mU^2}$, where Π_3 is a function of the front cornering stiffness and Π_4 is a function of the rear cornering stiffness.

2) Experimental Cornering Stiffness Estimation

Five sets of tires, differing in material and traction, are obtained and tested to determine the appropriate tires to use on the scale-model vehicle. A cornering stiffness testing apparatus has been designed and built allowing different types of tires to be tested at different speeds. The cornering stiffness testing apparatus in Fig. 4 consists of a movable arm, base, hub and axle assembly, vertical shaft, an optical encoder, added mass to simulate tire loading, and a weight and pulley set to simulate the steering force. Another approach to cornering stiffness estimation is discussed in [3].

By definition, cornering stiffness is the quotient of the steering force and the slip angle. If the movable arm is forced to stay parallel with the direction of the treadmill surface movement, the angle at which the wheel is turned is equal to the slip angle. A US Digital S1 optical shaft encoder is used to measure this angle, and a weight set is used to measure the force. To accurately simulate the conditions under which the tires will be performing, the axle assembly uses the same bearings as the scale-model vehicle. Also, the added mass is included to simulate the loading on the tires of the scale-model vehicle.

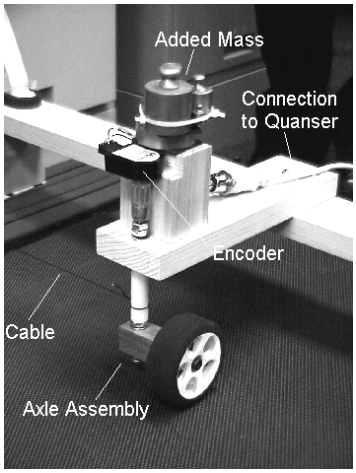

Fig. 4: Cornering stiffness testing apparatus

Since the optical encoder measures relative position, the encoder must be zeroed before the wheel angle can be measured. The slip angle is zero when the axle assembly is parallel to the base of the apparatus. Once the system is zeroed, the axle assembly is turned to the desired angle. As the treadmill is started, the movable arm attempts to turn in the direction of the wheel angle. To keep the movable arm in the correct position, weight is added incrementally to increase the force perpendicular to the direction of the wheel angle. When this force is great enough to move the wheel in the opposite direction of the wheel angle, the force is recorded. To obtain the cornering stiffness coefficient for one tire, this procedure is repeated in increments of 0.35 degrees from 0 to 3.5 degrees. The value of the cornering stiffness coefficient is the slope of the linear regression of the force and slip angle data.

Instead of testing each tire with the load correlating to the rear position, the rear cornering stiffness is determined using the ratio of the rear-axle loading to the front-axle loading. For the modified scale-model vehicle, this ratio is 0.694 and falls with the range of ratios for the full-size vehicles (0.582 to 0.871). Since the cornering stiffness is significantly correlated with normal load, the cornering stiffness of the rear tire can be approximated by multiplying the front cornering stiffness coefficient by 0.694. To verify that this method of approximating the rear cornering stiffness, one tire has been tested with both the front-axle loading and the rear-axle loading. With the front-axle loading, this tire has a cornering stiffness of 30.2 N/rad. With the rear loading, the cornering stiffness is reduced to 22.9 N/rad. Using the ratio to approximate the rear cornering stiffness, a value of 21.0 N/rad is calculated. The roughly 10% error is acceptable for this research and the rear cornering stiffness values for the other tires has been calculated using the ratio.

3) Buckingham-Pi Analysis of Cornering Stiffness Data

In calculating the Pi groups for the full-size vehicles, an empirical expression for the cornering stiffness from [11] was used in conjunction with vehicle parameters from [10]. Using this data, the front and rear cornering stiffness values have been calculated and Π_3 and Π_4 have been computed for a longitudinal velocity of 60 miles per hour (mph) and displayed in Table 1.

Using the experimental data, the tire with the smallest cornering stiffness was chosen to provide the best match between the Π_3 of the scale-model and full-size vehicles. For a full-size vehicle speed of 60 mph, the scale-model vehicle would have to travel at 16.8 mph (or 7.5 m/s).

IV. Vehicle Control Systems

The vehicle control system consists of the longitudinal and lateral control systems. The objective of these control systems is to regulate the position of the scale-model vehicle with respect to the treadmill. The longitudinal and lateral control systems use the information from the vision system to ensure that the vehicle remains in the center of the treadmill.

A. Longitudinal Control

The objective of the longitudinal control system is to regulate the longitudinal speed of the scale-model vehicle as determined by the speed of treadmill. In this case, the longitudinal control system tracks the desired speed by

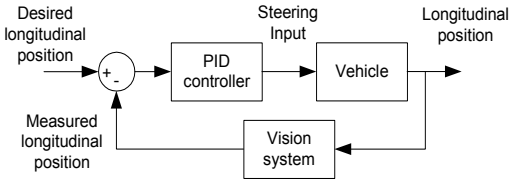

Fig. 5: Closed-loop system for control of longitudinal motion of scale-model vehicle

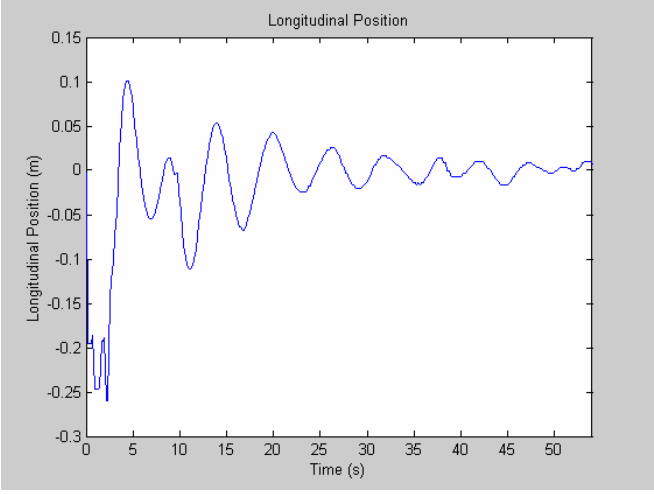

Fig. 6: Longitudinal position of the scale-model vehicle relative to the longitudinal center of the treadmill

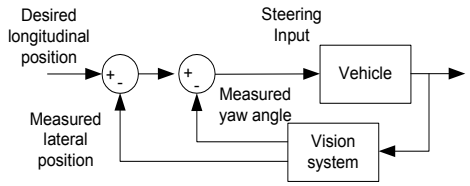

Fig. 7: Closed-loop system for state-feedback control of lateral motion of scale-model vehicle

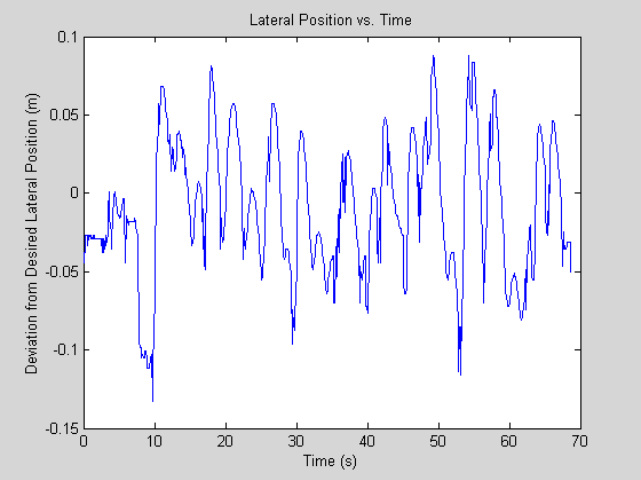

Fig. 8: Lateral position of the scale-model vehicle relative to the lateral center of the treadmill

regulating the longitudinal position of the vehicle to the longitudinal center of the treadmill surface in the camera's frame of reference. This configuration allows vehicles to be tested at constant or variable speeds. A block diagram of the longitudinal control system is shown in Fig. 5.

The vision system returns measurements of the vehicle's position on the treadmill surface. A PID controller was tuned experimentally to perform longitudinal control. Fig. 6 shows the experimental relative longitudinal position data. In this experiment, the treadmill is starting from rest and the longitudinal controller is following the speed of the treadmill as it accelerates to its steady-state speed.

B. Lateral Control

The objective of the lateral control system is to regulate the lateral position of the vehicle. The lateral controller uses measurements of the lateral position and heading to generate an appropriate steering input to the vehicle. Both state feedback and bang-bang lateral controllers have been considered. To this point, only preliminary results have been obtained. A summary of these efforts is presented in the sequel.

1) State feedback control

The state feedback controller design is based on the four state, bicycle model [8]. The state variables are the lateral position and velocity and the yaw angle and rate. The numerical state-space model is obtain using the parameters identified for the modified, scale-model vehicle. To obtain

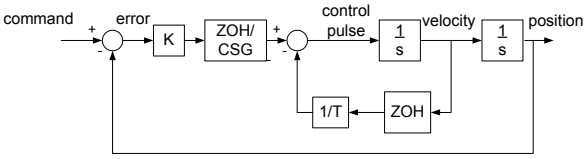

Fig. 9: Closed-loop block diagram of bang-bang control system

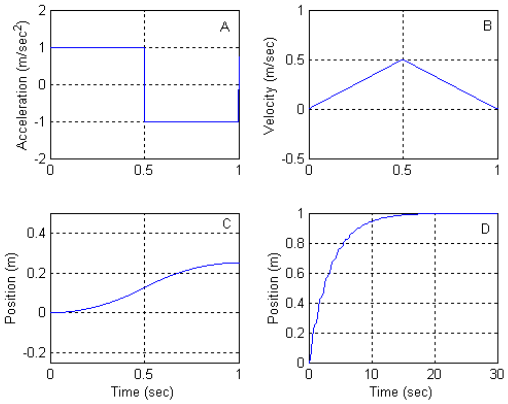

Fig. 10: Signals in the double integrator control system: (A) one period of the control input, (B) one period of the velocity response, (C) one period of the position response, (D) total position response

preliminary result, a very simple control law has been used

$$\delta = (y_d - y) + (\psi_d - \psi)$$

where δ is the steering input, y (resp. y_d) is the measured (resp. desired) lateral position and ψ (resp. ψ_d) is the measured (resp. desired) yaw angle. The closed-loop system is shown in Fig. 7. While this control law delivered good performance in simulation, the experimental performance was marginal. Fig. 8 shows the experimental relative lateral position data where the longitudinal controller regulates the vehicle's speed.

2) Bang-bang control

As an alternative to the state-space controller, a bang-bang lateral controller has been developed using results on bang-bang control of double integrator systems [12]. The lateral vehicle dynamics contain a double integrator as well as additional left-half-plane poles and zeros. As a result, the methods in [12] were modified to accommodate for the additional, stable dynamics [13].

The bang-bang control system for a double integrator system is shown in Fig. 9. The control strategy incorporates minimum-time control concepts in a closed-loop system. The bang-bang samples the tracking error using a zero-order hold (ZOH) and the control signal generator (CSG) produces a pre-determined control signal as shown in Fig. 10A. The control signal defines the desired inter-sample position and velocity behavior shown in Figs. 10B and 10C and generalizes the constant inter-sample behavior associated with a zero-order hold. Fig. 10D shows the position response of the closed-loop system to a step

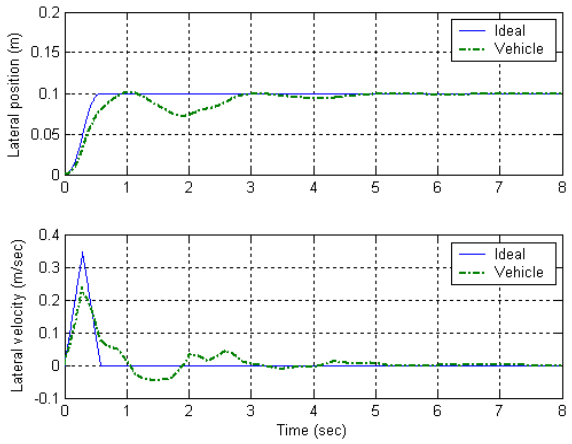

Fig. 11: Comparison of ideal double integrator and vehicle responses

command. The velocity feedback is required to account for a non-zero initial velocity or, for the vehicle, a non-zero initial yaw angle.

A simplified, steady-state model of the lateral dynamics (see [14])

$$\dot{\psi} = \frac{V}{L}\delta, \dot{y} = V\psi$$

allows the lateral control problem to be formulated as a double integrator control problem. Matching the steady-state vehicle model to the diagram in Fig. 9, the control input is the steering angle, the lateral position is the output and the yaw angle is proportional to the lateral velocity. Therefore, a steering input in the form of Fig. 10A produces a change in the lateral position and yaw angle as shown in Fig. 10 B and C, respectively, between samples of the lateral position tracking error. These motions result in the lateral position change shown in Fig. 10D.

To evaluate the performance of the bang-bang controller, the numerical model created from the identified scale-model vehicle parameters is used. Preliminary simulation results are shown in Fig. 11. The plot provides a comparison of the response of the ideal (double integrator) model and the modified scale-model vehicle model that consists of two integrators, two real stable poles, and two minimum-phase zeros. The bang-bang controller successfully regulates the lateral position. Due to the nature of the control input, the yaw angle is proportional to the lateral velocity in Fig. 11 and is completely determined by the lateral position command.

V. Conclusion

In this paper, the development of the Scale-Model Testing Apparatus (SMTA) at the United States Naval Academy is presented. This apparatus is a simplified version of a scale-model vehicle simulator developed at the University of Illinois. The SMTA incorporates off-the-shelf components and commercially available, scale-model vehicles which facilitates the development of the apparatus for an undergraduate setting. An overhead vision system provides a tether-free assessment of the vehicle's position and orientation. Dynamic similitude between the scale-model vehicle and an "average" full-size vehicle is achieved through a series of straightforward modifications to the scale-model vehicle. Preliminary results of longitudinal and lateral control designs are presented.

Currently, a new treadmill simulator is being developed to incorporate treadmill speed control and a faster vision system. Using the new apparatus, the scale-vehicle model will be verified through experimental system identification and the bang-bang lateral control design will be investigated. Moreover, the bang-bang steering input could be modified to incorporate input rate limits into the control system and be replaced by trapezoidal signals as in [8].

Acknowledgment

The authors are grateful to Andrew Alleyne and Sean Brennan from the University of Illinois for their support in developing this project.

References

[1] W. D. Jones, "Keeping Cars from Crashing," *IEEE Spectrum* vol. 38, no. 9 (2001): 40.

[2] T. A. McMahon and J. T. Bonner, *On Size and Life*. New York: Scientific American Library (1983).

[3] S. Brennan and A..Alleyne, "The Illinois Roadway Simulator: A Mechatronic Testbed for Vehicle Dynamics and Control," *IEEE Trans..Mechatronics*, vol. 5, pp. 349-359, Dec. 2000.

[4] S. Brennan and A. Alleyne, "Using a Scale Testbed: Controller Design and Evaluation," *IEEE Control Systems Mag*, June 2001.

[5] S. Brennan and A. Alleyne, "H-infinity Vehicle Control Using Non-Dimensional Perturbation Measures," in *Proc. American Control Conference,* Anchorage, AK, 2002, pp. 2534–2539.

[6] S. Burns, R. O'Brien, Jr., and J. Piepmeier, "Driver Assistance Steering Control Compensation of Accelerating Vehicle Motion", in *Proc. Southeastern Symposium Systems Theory*, Huntsville, AL, 2002, pp. 476-478.

[7] P. Hoblet, R. O'Brien, Jr., and J. Piepmeier, "Scale Model Vehicle Analysis for the Design of Steering Controller," in Proc. Southeastern Symposium Systems Theory, Morgantown, WV, 2003, pp. 201-205.

[8] H. Peng and M. Tomizuka, "Vehicle Lateral Control for Highway Automation," in *Proc. American Control Conference,* San Diego, 1990, pp. 788–794.

[9] A. Y. Maalej, D. A. Guenther and J. R. Ellis, "Experimental development of tyre force and moment models," *Intl. J. Vehicle Design*, vol. 10, 1989.

[10] R. Allen, H. Szostak, D. Klyde, T. Rosenthal, and K.Owens, *Vehicle Dynamic Stability and Rollover*, Springfield, VA: National Highway Traffic Safety Administration, 1992, pp. E7-47.

[11] R. W. Allen , H. T. Szostau, and T. J. Rosenthal, "Steady State and Transient Analysis of Ground Vehicle Handling," SAE Paper No. 870498, Feb. 1987.

[12] R. O'Brien, Jr., E. Boernke, and L. Gorsky, "Sampled data Control of Double Integrator Systems," in *Proc. Southeastern Symposium Systems Theory*, Morgantown, WV, 2003, pp. 413-416.

[13] C. George and R. O'Brien, Jr., "Vehicle Lateral Control using a Double Integrator Control Strategy," in *Proc. Southeastern Symposium Systems Theory*, Atlanta, 2004, to be published.

[14] J. Wong, *Theory of Ground Vehicles* . New York: Wiley, 2001, pp. 350-352.